

Thermochemistry and Conformational Polymorphism of a Hexamorphic Crystal System

Lian Yu,^{*,†} Gregory A. Stephenson,[†] Christine A. Mitchell,[†] Charles A. Bunnell,[‡] Sharon V. Snorek,[‡] J. Joe Bowyer,[‡] Thomas B. Borchardt,^{§,#} Joseph G. Stowell,[§] and Stephen R. Byrn^{*,§}

Contribution from the Lilly Research Laboratories, Eli Lilly and Company, Lilly Corporate Center, Indianapolis, Indiana 46285, Eli Lilly and Company, Tippecanoe Laboratories, Lafayette, Indiana 47902, and Department of Industrial & Physical Pharmacy, Purdue University, West Lafayette, Indiana 47907-1336

Received August 23, 1999

Abstract: 5-Methyl-2-[(2-nitrophenyl)amino]-3-thiophenecarbonitrile has been crystallized as six solvent-free polymorphs, which differ in the mode of packing and in molecular conformation. The conformational difference results principally from the thiophene torsion relative to the *o*-nitroaniline fragment, which leads to different crystal colors (red, orange, and yellow). Thermodynamic stability relationships between polymorphs have been determined from solid-state conversions and calorimetric data of melting and eutectic melting. Vibrational spectroscopy and ab initio calculations showed that most conformers in solution feature perpendicularly arranged thiophene and *o*-nitroaniline fragments, although a minor population of more planar conformers also exist. Crystallization has a stabilizing effect for more planar and higher dipole conformers over perpendicular ones by 3–6 kJ/mol. The only exception to this pattern is the one polymorph containing weak intermolecular hydrogen bonds.

Introduction

Polymorphism, the ability of a molecule to adopt different crystal forms, is an important phenomenon for the study of structure–property relationships,^{1–5} the effect of crystal forces on molecular conformation,^{6–8} molecular-level control of crystallization,^{9–12} and the prediction¹³ and design¹⁴ of crystal structures. Systems having many polymorphs are beneficial to such studies, because they allow broader explorations of the

potential energy hypersurface along intra- and intermolecular coordinates. We report here that 5-methyl-2-[(2-nitrophenyl)amino]-3-thiophenecarbonitrile (C₁₂H₉N₃O₂S, **1**, Figure 1) produces at least six solvent-free polymorphs, all of which are sufficiently stable to permit X-ray structural determination at room temperature. This degree of polymorphism is unusual with respect to current entries in the Cambridge Structural Database. Our survey in May 1999, conducted in a manner similar to that of the 1995 survey by Gavezzotti and Fillippini,¹ found 321 polymorphic systems composed of C, H, N, O, F, Cl, and S, in which 291 are dimorphic, 27 trimorphic, three have four polymorphs, and none have five or more.¹⁵ Besides extensive polymorphism, an interesting aspect of **1** is its ability to adopt significantly different conformations in different polymorphs (conformational polymorphism),⁶ which lead to color and other spectral differences between polymorphs.^{16,17}

This study focuses on the relative thermodynamic stability of the polymorphs of **1**. Unlike previous studies of conformational polymorphism that rely on force-field derived crystal energies,^{6–8} we directly measured free-energy differences between polymorphs, thus accounting for both energy and

* To whom correspondence should be addressed.

† Lilly Research Laboratories, Eli Lilly & Company, Lilly Corporate Center.

‡ Eli Lilly & Company, Tippecanoe Laboratories.

§ Department of Industrial & Physical Pharmacy, Purdue University.

#Current address: G. D. Searle Pharmaceuticals, PDAD Department, 4901 Searle Parkway, Skokie, IL 60077-2980.

(1) Gavezzotti, A.; Fillippini, G. *J. Am. Chem. Soc.* **1995**, *117*, 12299–12305.

(2) Dunitz, J. D. *Acta Crystallogr.* **1995**, *B51*, 619–631.

(3) Jacques, J.; Collet, A.; Wilen, S. H. *Enantiomers, Racemates, and Resolutions*. Krieger Publishing Company: Malabar, Florida, 1991.

(4) Brock, C. P.; Schweizer, W. B.; Dunitz, J. D. *J. Am. Chem. Soc.* **1991**, *113*, 9811–9820.

(5) Bernstein, J. *J. Phys. D: Appl. Phys.* **1993**, *26*, B67–76.

(6) Bernstein, J. Conformational Polymorphism. In *Organic Solid State Chemistry*; Desiraju, G. R., Ed.; Elsevier: Amsterdam, 1987 and references therein.

(7) Buttar, D.; Charlton, M. H.; Docherty, R.; Starbuck, J. *J. Chem. Soc., Perkin Trans.* **1998**, *2*, 763–772.

(8) Starbuck, J.; Docherty, R.; Charlton, M. H.; Buttar, D. *J. Chem. Soc., Perkin Trans.* **1999**, *2*, 677–691.

(9) Staab, E.; Addadi, L.; Leiserowitz, L.; Lahav, M. *Adv. Mater.* **1990**, *2*, 40.

(10) Davey, R. J.; Blagden, N.; Potts, G. D.; Docherty, R. *J. Am. Chem. Soc.* **1997**, *119*, 1767–1772.

(11) Bonafede, S.; Ward, M. *J. Am. Chem. Soc.* **1995**, *117*, 7853–7861.

(12) Bernstein, J.; Davey, R. J.; Henck, J.-O. *Angew. Chem., Int. Ed.* **1999**, *38*, 3441–3461.

(13) Gavezzotti, A. *Acc. Chem. Res.* **1994**, *27*, 7153–7157.

(14) Desiraju, G. R. *Crystal Engineering The Design of Organic Solids*. Elsevier: New York 1989.

(15) See Supporting Information. Gavezzotti and Fillippini found 163 polymorphic systems whose structures have been solved at the room temperature, in which 13 have three polymorphs, three have four, and none have five or more. Reports of extensive polymorphism can be found in the thermomicroscopy literature (for example, Kuhnert-Brandstatter, M. *Thermomicroscopy in the analysis of pharmaceuticals*. Oxford: Pergamon Press, 1971). However, some are transient phases observed during heating or cooling without crystallographic conformation. The polymorphism of **1** is distinguished by the number of polymorphs that are stable essentially indefinitely at the room temperature to allow crystallographic and other analyses.

(16) Stephenson, G. A.; Borchardt, T. B.; Byrn, S. R.; Bowyer, J.; Bunnell, C. A.; Snorek, S. V.; Yu, L. *J. Pharm. Sci.* **1995**, *84*, 1385–1386.

(17) Smith, J.; MacNamara, E.; Raftery, D.; Borchardt, T.; Byrn, S. J. *Am. Chem. Soc.* **1998**, *120*, 11710–11713.

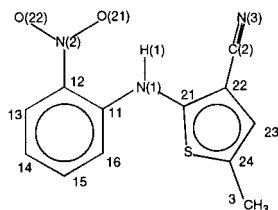


Figure 1. Molecular structure and atomic designations of **1**.

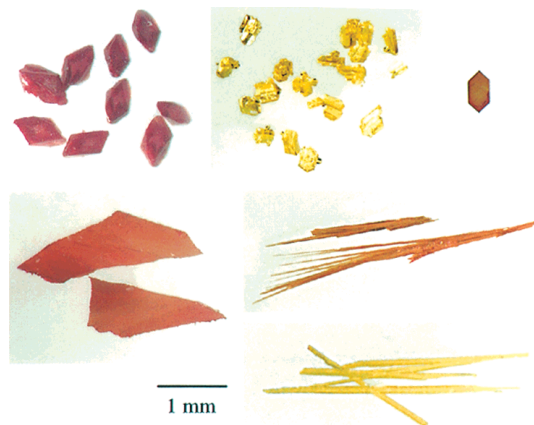


Figure 2. Photomicrographs of the polymorphs of **1**, showing different habits and colors. From upper left, clockwise: R, Y, OP, ON, YN, ORP.

entropy contributions to crystal stability. The entropy effect, although unimportant at 0 K, is necessary to treat enantiotropism, a commonly observed¹⁸ phenomenon in which the stability order of polymorphs changes with temperature. To characterize the effect of crystal forces on molecular conformation, we also determined the conformation of **1** in solutions by vibrational spectroscopy and ab initio calculations.

Experimental Section

The synthesis of **1**¹⁹ and the preparation of its polymorphs were carried out at Eli Lilly and Company. Six solvent-free polymorphs have been identified (Figure 2): Form R (red prisms, mp 106.2 °C), Form Y (yellow prisms, mp 109.8 °C), Form OP (orange plates, mp 112.7 °C), Form ON (orange needles, mp 114.8 °C), Form YN (yellow needles, mp not measurable because of thermal instability), and Form ORP (orange-red plates, mp not measurable because of thermal instability).²⁰ The crystallization of **1** showed poor polymorphic selectivity. For example, all polymorphs (occasionally mixtures) have been obtained from methanol solutions, and several polymorphs could nucleate simultaneously (“concomitant polymorphs”)¹² from a supercooled melt.

Because of this poor selectivity, we can provide only rough guidelines for polymorph preparation: Y was produced by solution-mediated (“slurry”) conversion of any other form near room temperature; fast crystallization favored the needlelike ON and YN; although obtainable by heating R, solution-grown OP was obtained only with seeding and tended to crystallize with ON; YN tended to crystallize first as spherulites from a supercooled melt between a slide and a cover glass.

Crystal data for Forms Y, ON, OP, and R were collected using an Enraf-Nonius CAD4 diffractometer with graphite-monochromated Mo K α radiation ($\lambda = 0.71069$ Å). Crystal data for Forms YN and ORP were collected using a Siemens P4 diffractometer equipped with a

(18) Burger, A.; Ramberger, R. *Mikrochim. Acta [Wien]* **1979**, *II*, 259–271 and 273–316.

(19) Lilly Industries Limited, Kingsclere Road, Basingstoke Hants RG21 2XA (UK), Eur. Pat. 0 454 436 A1, Oct 10, 1991, Bulletin 91/44; Callogaro, D. O.; Fairhurst, J.; Hotten, T. M.; Moore, N. A.; Tupper, D. E. *Bioorg. Med. Chem. Lett.* **1997**, *7*, 25–30.

(20) Previously (ref 16), we designated Form ON simply as O, because Form OP, also orange-colored, was then unknown.

SMART 1000 CCD area detector with Cu K α radiation ($\lambda = 1.54184$ Å). Lorentz and polarization corrections were applied to the data. No absorption correction was made, except for Forms ON and OP, where an empirical absorption correction based on the method of Walker and Stuart was applied.²¹ Structures were solved by means of direct methods (SHELX-86²² for Y, ON, OP, YN, and ORP; SIR88²³ for R) and refined using full matrix least-squares procedures (MoLEN²⁴ for Y, R, and ON; SHELX-93²⁵ for OP, YN, and ORP). Scattering factors were taken from Cromer and Waber.²⁶ All non-hydrogen atoms were refined anisotropically. The hydrogen atoms of Forms Y, R, and ON were located in the difference map and added to the structure factor calculations, but their positions were not refined, except as noted in Supporting Information. For Form OP, the hydrogen atoms were located in successive difference maps and refined with a riding model, and hydrogens of Forms YN and ORP were located and refined isotropically. Additional details of the crystallographic analyses are given in Table 1 and the Supporting Information. X-ray powder diffraction (XRD) was conducted using a Siemens Diffraktometer D5000.

IR absorption spectra were recorded using an IR microscope (Nicolet 60SXB). Solution IR spectra were recorded in carbon tetrachloride. IR spectra of the supercooled melt were recorded at room temperature through a liquid layer between two polished KBr disks produced by melting. The melt preparation was also used to record spectra of thin crystals after recrystallization, usually with enhanced spectral resolution. Raman spectra were recorded using a Nicolet Magna 950 FT Raman spectrometer with Nd:YAG laser excitation (1.064 μm). Backscattered radiation was collected from crystals packed in glass capillary tubes.

Differential scanning calorimetry (DSC) was conducted in crimped aluminum pans using a Seiko DSC 210 under 50 mL/min nitrogen purge. From the melting data of two polymorphs, i and j, the free energy and entropy differences were calculated by:²⁷

$$(G_j - G_i)_{T_{mi}} = \Delta H_{mj}(T_{mi} - T_{mj})/T_{mj} + \Delta C_{pmj}[T_{mj} - T_{mi} - T_{mi} \ln(T_{mj}/T_{mi})] \quad (1)$$

$$(S_j - S_i)_{T_{mi}} = \Delta H_{mi}/T_{mi} - \Delta H_{mj}/T_{mj} + \Delta C_{pmj} \ln(T_{mj}/T_{mi}) \quad (2)$$

where T_{mi} and T_{mj} are the melting points of i and j, ΔH_{mi} and ΔH_{mj} their enthalpies of melting, and ΔC_{pmj} the heat capacity change upon melting j (estimated from the baseline shift across melting endotherms). The subscript T_{mi} signifies that $(G_j - G_i)$ and $(S_j - S_i)$ are evaluated at T_{mi} . Equations 1 and 2 thus provide the segment of the $(G_j - G_i)$ vs T curve at T_{mi} : eq 1, the value, and eq 2, the temperature slope $[d(G_j - G_i)/dT = -(S_j - S_i)]$.

Eutectic melting of the polymorphs was measured by DSC against common reference compounds (RC), including acetanilide, benzil, azobenzene, and thymol, which were chosen²⁸ to reduce the melting points of **1** by different degrees. The data thus recorded were used to calculate $(G_j - G_i)$ at eutectic melting temperatures:

$$x_{ej}(G_j - G_i)_{T_{ei}} = \Delta H_{mej}(T_{ei} - T_{ej})/T_{ej} - \Delta C_{pej}[T_{ei} - T_{ej} - T_{ei} \ln(T_{ei}/T_{ej})] + RT_{ei}\{x_{ej} \ln(x_{ej}/x_{ei}) + (1 - x_{ej}) \ln[(1 - x_{ej})/(1 - x_{ei})]\} \quad (3)$$

where T_{ei} and T_{ej} are the eutectic melting points of i and j with a common RC, x_{ei} and x_{ej} the eutectic compositions, ΔH_{mei} and ΔH_{mej} enthalpies of eutectic melting, ΔC_{pej} the heat capacity change upon

(21) Walker, N.; Stuart, D. *Acta Crystallogr.* **1983**, *A39*, 158.

(22) Sheldrick, G. M. *SHELXS86: A Program for the Solution of Crystal Structures*; University of Göttingen: Germany, 1985.

(23) Burla, M. C.; Camilli, M.; Cascarano, G.; Giacovazzo, C.; Polidori, G.; Spagna, R.; Viterbo, D. *J. Appl. Cryst.*, **1989**, *22*, 389.

(24) Fair, C. K. *MoLEN Structure Determination System*, Delft Instruments: Delft, The Netherlands, 1990.

(25) Sheldrick, G. M. *SHELXS93: Program for crystal structure refinement*; Institute für Anorg Chemie: Göttingen, Germany, 1993.

(26) Cromer, D. T.; Waber, J. T. *International Tables for X-ray Crystallography*; The Kynoch Press: Birmingham, England, 1974; Vol. IV, Table 2.2B.

(27) Yu, L. J. *Pharm. Sci.*, **1995**, *84*, 966–974.

(28) McCrone, W. C. *Fusion Methods in Chemical Microscopy*; Interscience Publishers: New York, 1957.

Table 1. Crystal Data and Data Collection Parameters^a

form	Y	ON	OP	R	YN	ORP
crystal system	monoclinic	monoclinic	monoclinic	triclinic	triclinic	orthorhombic
space group [No.]	$P2_1/n$ [14]	$P2_1/c$ [14]	$P2_1/n$ [14]	$P\bar{1}$ [2]	$P\bar{1}$ [2]	$Pbca$ [61]
description	yellow prism	orange needle	orange plate	red prism	yellow needle	orange-red plate
crystal size, mm	$0.49 \times 0.47 \times 0.25$	$0.30 \times 0.15 \times 0.08$	$0.27 \times 0.22 \times 0.13$	$0.25 \times 0.13 \times 0.10$	$0.04 \times 0.075 \times 0.5$	$0.1 \times 0.2 \times 0.3$
<i>a</i> , Å	8.5001(8)	3.9453(7)	7.9760(9)	7.4918(5)	4.5918(8)	13.177(3)
<i>b</i> , Å	16.413(2)	18.685(1)	13.319(2)	7.7902(5)	11.249(2)	8.0209(18)
<i>c</i> , Å	8.5371(5)	16.3948(4)	11.676(1)	11.9110(8)	12.315(2)	22.801(5)
α , °	90	90	90	75.494(6)	71.194(3)	90
β , °	91.767(7)	93.830(5)	104.683(8)	77.806(6)	89.852(4)	90
γ , °	90	90	90	63.617(6)	88.174(3)	90
volume, Å ³	1190.5(4)	1205.9(3)	1199.9(4)	598.88(7)	601.85(19)	2409.8(9)
<i>Z</i>	4	4	4	2	2	8
D_{calcd} , g cm ⁻³	1.447	1.428	1.435	1.438	1.431	1.429
<i>T</i> , K	293	293	295	293	296	296
radiation ^b	Mo K α	Cu K α	Cu K α	Cu K α	Mo K α	Mo K α
μ , mm ⁻¹	0.256	2.33	2.34	2.35	0.266	0.265
<i>F</i> (000)	536.0	536.0	536.0	268.0	268.0	1072
reflns collected	2095	2629	2612	2298	4239	15904
unique reflns	1956	2283	2437	2184	2690	2888
<i>R</i>	0.033	0.042	0.049	0.037	0.050	0.051
R_w ^c	0.044	0.055	0.122	0.050	0.100	0.106
GOF	1.415	1.392	1.000	1.428	0.839	0.757

^a Empirical formula: C₁₂H₉N₃O₂S. MW: 259.29. ^b Mo K α (0.71073 Å), Cu K α (1.54184 Å).

Table 2. Selected Structural Parameters^a

form	Y	ON	OP	R	YN	ORP
C11–N1–C21–S (θ_{thio}), deg	104.7(2)	52.6(4)	46.1(4)	21.7(3)	104.1(3)	39.4(5)
C21–N1–C11–C12 (θ_{phen}), deg	–175.0(2)	–173.3(2)	–167.3(2)	–150.0(2)	–175.2(2)	–174.3(3)
O21–N2–C12–C11 (θ_{nitro}), deg	–1.8(3)	–4.4(4)	–18.7(4)	–18.4(3)	–3.6(4)	–3.5(5)
C24–S–C21–N1, deg	179.6(2)	172.1(2)	173.9(2)	174.0(2)	179.1(2)	173.8(3)
C–C \equiv N angle, deg	177.9(2)	176.2(3)	178.6(3)	178.6(2)	178.5(3)	177.4(4)
Amino C–N–C, deg	122.8(2)	126.1(2)	126.2(2)	126.3(1)	123.9(3)	129.6(4)
HN–C(thiophene), Å	1.401(2)	1.386(3)	1.389(3)	1.386(3)	1.401(3)	1.384(4)
HN–C(phenyl), Å	1.377(2)	1.380(3)	1.380(3)	1.381(2)	1.365(3)	1.371(4)
O ₂ N–C(phenyl), Å	1.446(2)	1.441(3)	1.445(4)	1.446(2)	1.447(3)	1.456(4)

^a One of the two mirror-related conformers ($\theta_{\text{thio}} > 0$) is described. Error in the last digit is indicated in parentheses.

melting the j-RC eutectic, and R the ideal gas constant. The subscript T_{ei} signifies that $(G_j - G_i)$ is evaluated at T_{ei} . Equation 3 can be derived under the ideal solution assumption through straightforward manipulations of thermodynamic equations. Briefly, the procedure involves constructing a thermodynamic cycle linking i and j that consists of eutectic melting, temperature change, and dissolution as intermediate steps. For the present system, the first of the three terms in eq 3 dominates. By symmetry, $(G_j - G_i)$ at T_{ei} is given by eq 3 upon exchanging i and j. The reference compounds were obtained from Aldrich and used without further purification.

Results and Discussions

Crystal Structures. Table 1 summarizes the crystallographic data for the six polymorphs of **1**. The structures of Y, ON, and R have been briefly described¹⁶ and those of OP, YN, and ORP are new. The molecules in different polymorphs differ significantly in the torsional angle C11–N1–C21–S (θ_{thio}); in the order $Y \sim YN > ON > OP > ORP > R$, θ_{thio} changes by 83° (Table 2), which brings the thiophene ring from being perpendicular to nearly coplanar to the amino group. Conformers Y and YN adopt essentially the same conformation. In addition to θ_{thio} , smaller changes are observed in other torsional angles: the phenyl torsional angles C21–N1–C11–C16 (θ_{phen}) differ by 25° among the polymorphs; the nitro group is twisted out of the phenyl plane by 18° in R and OP, but is approximately coplanar in other polymorphs. The conformational differences qualify Y and YN as conformational polymorphs of the other polymorphs according to the criterion: $\Delta I = (\Delta I_x^2 + \Delta I_y^2 +$

$\Delta I_z^2)^{1/2} > 10\%$, where ΔI_x , ΔI_y , and ΔI_z are percent changes in the three principal moments of inertia.¹⁶

Although most covalent bond lengths and angles do not change significantly between the polymorphs, some exceptions are observed (Table 2): the HN–C(thiophene) bond is significantly longer, and the amino C–N–C angle significantly smaller in Y and YN than in the other polymorphs; the C–C \equiv N angle deviates from 180° in several polymorphs, notably ON; the amino nitrogen is not always coplanar with the thiophene plane (see torsional angle C24–S–C21–N1), again most significantly in ON. Longer HN–C(thiophene) bond lengths in Y and YN correlate with the smaller π -conjugation between the thiophene and the amino lone pair in these conformers.

An intramolecular hydrogen bond exists between the nitro and amino groups in all polymorphs, as would be expected. The only good hydrogen bond donor thus engaged, one expects no intermolecular hydrogen bonds. This is indeed the case in all polymorphs but Y, in which the amino hydrogen makes a short contact with the cyano group of a neighboring molecule. The amino hydrogen of the (0,0,0) molecule approaches the cyano N of the (–1,0,–1) molecule with $d(\text{N}\cdots\text{N}) = 3.13$ Å, $d(\text{CN}\cdots\text{H}) = 2.42$ Å, and $\alpha(\text{N}–\text{H}\cdots\text{N}) = 140^\circ$.²⁹

All of the polymorphs have centrosymmetry, containing equal numbers of molecules of opposite chirality in the unit cells.

(29) We stated previously that hydrogen bonding is exclusively *intramolecular* (ref 16). However, reexamination of the structures revealed a weak intermolecular hydrogen bond in Form Y.

Apart from the intermolecular hydrogen bonds in Form Y, no intermolecular contacts or special packing motifs appear significant, which indicates that the primary mode of molecular association in these crystals is van der Waals (dispersion, dipole–dipole, etc.).

Thermochemistry. To determine the stability relationships between the polymorphs, we first obtained qualitative stability orders of the polymorphs through polymorphic conversions, which were monitored by X-ray powder diffraction and Raman spectroscopy. Melting and eutectic melting data were then used to determine quantitative differences between free energies, enthalpies, and entropies of polymorphs.

At room temperature, YN underwent conversions in hours to days. Well-formed, solution-grown crystals of YN converted to R and Y in days to weeks, beginning from the ends or cracks and showing a migration of phase boundaries along the needle axis. Melt-grown crystals of YN converted in hours to days to Y, ON, or R, seemingly without discrimination. ORP underwent a slow conversion at room temperature to Y (detectable in several days). Room-temperature transformation in R was observed only after years of storage, yielding isolated particles of OP or Y among the R crystals (confirmed by manual isolation followed by melting-point measurement). Y, ON, and OP remained unchanged at room-temperature indefinitely.

Assisted by saturated solutions, all other forms converted directly to Y between 20 and 60 °C in hours to days. Heating R in the dry state between 70 and 100 °C caused conversion to Y, OP, or ON in hours to days, seemingly without discrimination. These transformations resulted in pronounced color changes, and in the case of R to ON, growth of orange “whiskers” from the initially red, prism-like crystals. Although the R–Y and R–OP conversions led to no significant morphological changes, single-crystal X-ray diffraction and light microscopy showed that these transitions produced microcrystalline particles and occurred through migrations of phase boundaries. Heating Y at 95 °C caused a slow conversion (days to weeks) to a mixture of ON and OP, which was accelerated upon grinding the crystals. Y also converted to ON in an ethylene glycol slurry at 90 °C, producing fiberlike orange crystals. OP and ON remained unchanged at 90–100 °C for weeks.

At 10 °C/min heating rate, four polymorphs (Y, ON, OP, and R) melted as pure phases, without any solid–solid transformation (Figure 3). YN and ORP, on the other hand, underwent rapid solid-state conversion near 70 °C, making it impossible to measure their melting points. Figure 4 shows the DSC feature of a YN sample, which converted exothermically to Y and R (trace amount) before melting. In other samples of YN, conversion to ON was also observed. Heating ORP caused conversion to ON or Y.

The polymorphic conversions described above indicate a complex relationship between the polymorphs. For example, Form Y is the most stable at 20–60 °C, but less stable than Forms OP and ON at a higher temperature (enantiotropy). Form R is always less stable than Form Y above room temperature.

Figure 5 illustrates the use of melting and eutectic melting data for determining the stability relationship between polymorphs, in this case between Y and ON. Near the melting region, the high-melting ON is more stable than Y. Upon successively reducing their melting points by the addition of reference compounds, the melting order changed from ON > Y (acetanilide), to ON \approx Y (benzil), and to ON < Y (azobenzene and thymol). Thus, the stability order of ON and Y reverses at approximately 70 °C. The curve above the DSC data represents the free-energy difference between ON and Y

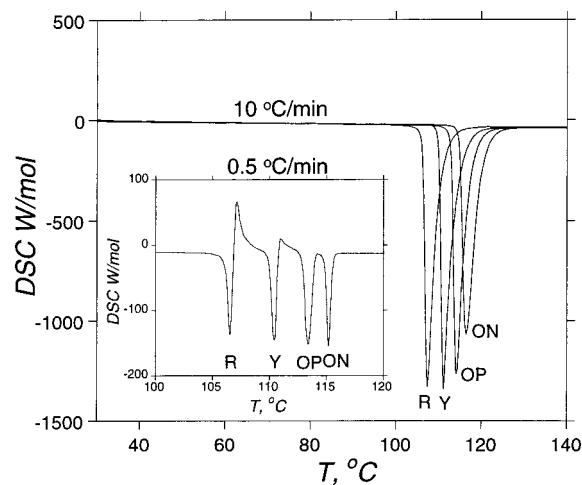


Figure 3. Melting endotherms of Forms R, Y, OP, and ON (left to right) recorded at 10 °C/min, each showing the homogeneous melting of a unique polymorph. Inset: DSC trace recorded at 0.5 °C/min of a polymorphic mixture, showing better separated melting endotherms and exotherms caused by crystallization from supercooled melt.

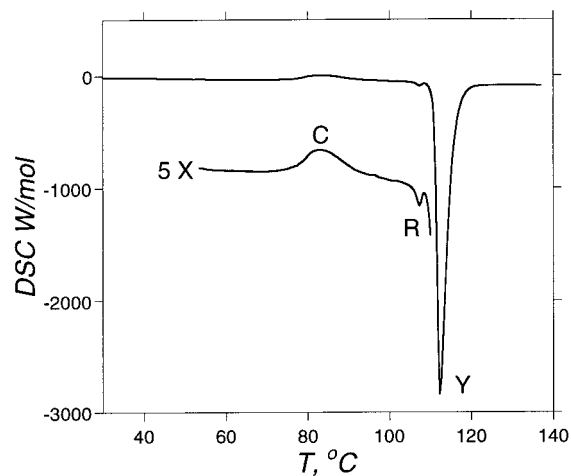


Figure 4. DSC trace of a sample of YN showing an exothermic conversion (Event C) and subsequent melting as R (trace amount) and Y. The area of C gives an estimate of the enthalpy difference of YN and Y. This experiment used a faster-than-normal heating rate (20 °C/min) in an (unsuccessful) attempt to observe the pure melting of YN. The faster rate caused thermal events to be more intense than those seen in Figure 3.

calculated by eqs 1–3. The segment near the pure melting points was obtained from eqs 1 (value) and 2 (slope). The individual points were calculated using eq 3. The Y and ON lines terminate at the liquid line (L, stable liquid; L-sc supercooled liquid).

Figure 6 shows the stability relationships between the polymorphs obtained from melting and eutectic melting data (Table 3). Table 4 summarizes the entropy and enthalpy differences between the polymorphs, which were calculated from the slopes of the $\Delta G - T$ and $\Delta G/T - 1/T$ plots, respectively. Because some curvature is present in curve R, the two lowest-temperature data points (from the thymol eutectics) were omitted from slope calculations. Because of poor thermal stability, YN showed eutectic melting with only thymol, the lowest-melting reference compound. Otherwise, YN first underwent solid-state conversions and then showed eutectic melting as a more stable polymorph. The line YN in Figure 6 was constructed from the thymol-eutectic data and the enthalpy of the YN-to-Y conversion (Figure 4).³⁰ The melting/eutectic melting data of ORP have not been measured because of scarcity of material.

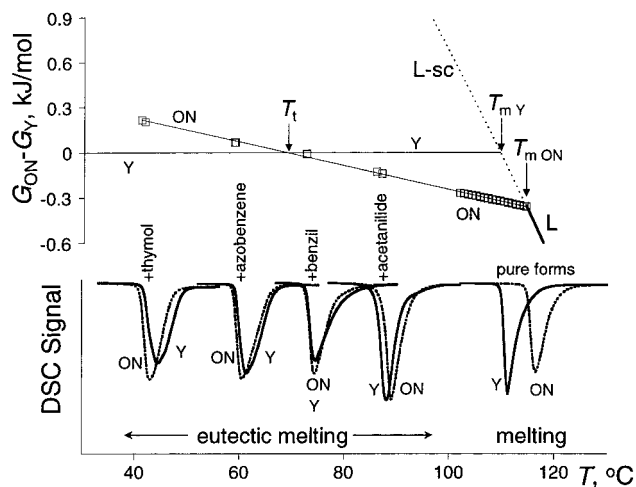


Figure 5. Illustration of the use of melting and eutectic data for determining the stability relationship between polymorphs. Bottom: melting endotherms of Y and ON as pure crystals and in the eutectics with acetanilide, benzil, azobenzene, and thymol. Top: the $\Delta G - T$ curve calculated using eqs 1–3. The free energy of ON is plotted against that of Y (horizontal line). The ON and Y lines terminate at the liquid line (L: stable liquid, L-sc: supercooled liquid).

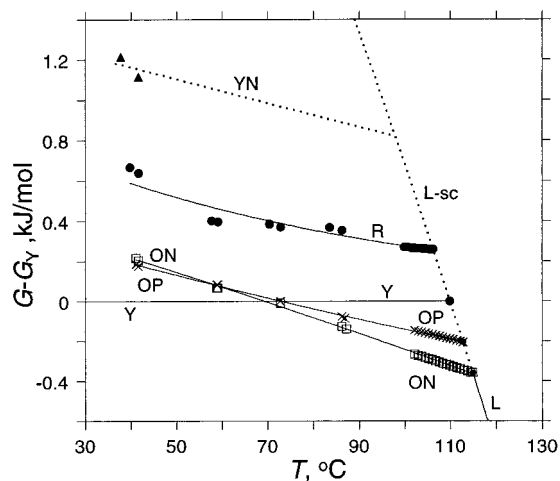


Figure 6. Stability relationship between polymorphs constructed from melting and eutectic melting data. Each line represents the free energy of a polymorph relative to Y (i.e., $G - G_Y$).

Solution Conformations. To understand the effect of crystallization on molecular conformation, we investigated the conformational preference of **1** in solution by vibrational spectroscopy and ab initio calculations. Figure 7 shows the CN stretch region of the vibrational spectrum. The solution spectrum (recorded in CCl_4) features a dominant peak at high frequency and a red-shifted shoulder, in contrast to the sharp and symmetrical crystal spectra. Since the CN stretch frequency ν_{CN} of an aromatic nitrile depends on the adjacent substituent (increased by electron acceptors and decreased by electron donors),³¹ the ν_{CN} of **1** is expected to be the highest near $\theta_{\text{thio}} \approx 90^\circ$, where the amino perturbation is the weakest, and to decrease as θ_{thio} approaches 0 or 180° , where the amino perturbation is the strongest. With the exception of YN, this trend holds: in the order Y, ON, OP, ORP, and R, θ_{thio} decreases

(30) The enthalpy of conversion ($H_{\text{YN}} - H_{\text{Y}} = 3.0$ kJ/mol provides the temperature slope $d(G_{\text{YN}} - G_{\text{Y}})/dT = -(H_{\text{YN}} - H_{\text{Y}}) - (G_{\text{YN}} - G_{\text{Y}})/T$.

(31) ν_{CN} is 2229 cm^{-1} in benzonitrile, 2238 cm^{-1} in *o*-fluorobenzonitrile, and 2213 cm^{-1} in *o*-aminobenzonitrile (Pouchert, C. J. *The Aldrich Library of FT-IR Spectra*; Aldrich Chemical Co.: Milwaukee, 1985).

Table 3. Melting and Eutectic Melting Data^a

form	Y	ON	OP	R	YN
Melting					
$T_m, ^\circ\text{C}$	109.8	114.8	112.7	106.2	(98) ^b
$\Delta H_m, \text{kJ/mol}$	27.2	25.1	25.5	26.0	(24.2) ^b
Eutectic Melting					
RC = acetanilide					
x_e	0.47	0.46	0.47	0.50	-
$T_e, ^\circ\text{C}$	86.28	87.28	86.89	83.51	-
$\Delta H_{me}, \text{kJ/mol}$	23.2	21.5	21.5	22.2	-
RC = benzil					
x_e	0.38	0.38	0.38	0.41	-
$T_e, ^\circ\text{C}$	72.72	72.78	72.71	70.39	-
$\Delta H_{me}, \text{kJ/mol}$	22.7	21.7	21.7	21.7	-
RC = azobenzene					
x_e	0.22	0.22	0.22	0.25	-
$T_e, ^\circ\text{C}$	59.09	58.86	58.81	57.65	-
$\Delta H_{me}, \text{kJ/mol}$	21.8	21.5	21.5	21.2	-
RC = thymol					
x_e	0.15	0.16	0.16	0.18	0.22
$T_e, ^\circ\text{C}$	41.64	41.05	41.13	39.74	37.74
$\Delta H_{me}, \text{kJ/mol}$	17.6	16.6	16.6	17.3	15.8

^a RC = reference compound. The second decimal place of T_e has been included to preserve the precision of the differences between eutectic temperatures, which was approximately ± 0.03 $^\circ\text{C}$, even though the accuracy of these temperatures, limited by indium calibration, was ± 0.1 $^\circ\text{C}$. ^b T_m obtained by extrapolating the G_{YN} curve to the liquid curve (Figure 6). ΔH_m obtained by subtracting the energy of conversion from ΔH_m of Form Y.

Table 4. Thermodynamic Parameters^a

forms	$\Delta H, \text{kJ/mol}$	$\Delta S, \text{J/K/mol}$	$T_i, ^\circ\text{C}$
Y = LT ON = HT	2.6	7.7	70
Y = LT OP = HT	1.9	5.3	72
Y = S R = MS	1.4	3.0	<i>c</i>
Y = S YN = MS	3.0 ^b		<i>c</i>

^a Enantiotropic systems: LT = low-temperature form, HT = high-temperature form. Monotropic systems: S = stable form, MS = metastable form. ^b From YN–Y enthalpy of conversion. ^c $T_i > T_m$ (virtual transition temperature of monotropic polymorphs).

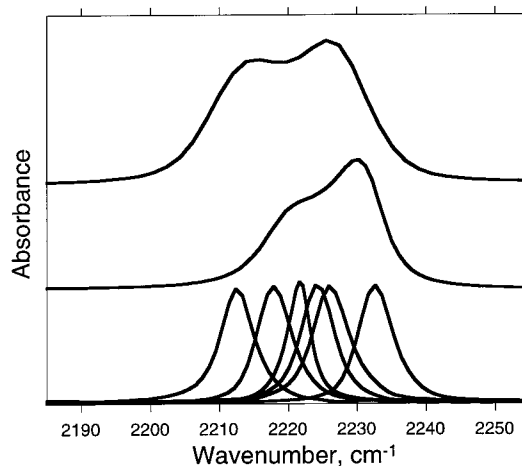


Figure 7. The CN stretch bands of **1**. Bottom (left to right): Forms R, ORP, YN, ON, OP, and Y. Middle: CCl_4 solution (0.90 mM). Top: supercooled melt at 22 $^\circ\text{C}$.

and so does ν_{CN} . Thus, the solution spectrum implies that solution conformers are predominantly perpendicular ($\theta_{\text{thio}} \approx 90^\circ$), although a significant population of nonperpendicular conformers is also present.

Conformer YN does not conform to the $\nu_{\text{CN}} - \theta_{\text{thio}}$ correlation: although conformers Y and YN are virtually identical, the ν_{CN} of YN is approximately 10 cm^{-1} lower than that of Y. This may result from the different chemical environment of the

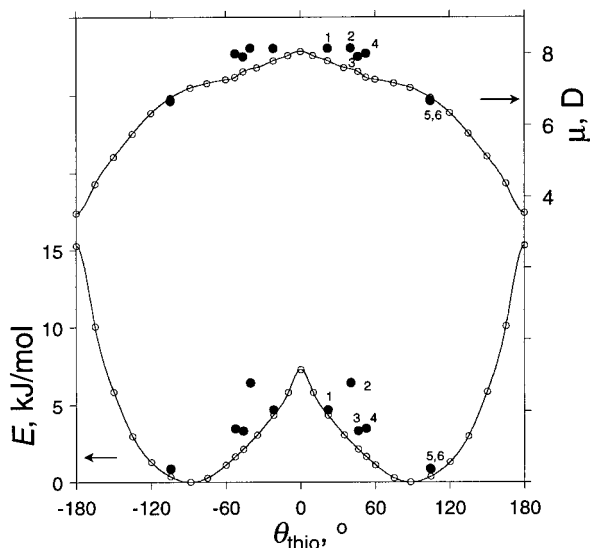


Figure 8. Conformational energy (bottom) and dipole moment (top) as a function of θ_{thio} , calculated at the RHF/6-31G* level. Solid circles correspond to conformers observed in crystals: 1-R, 2-ORP, 3-OP, 4-ON, 5-Y, 6-YN.

CN group in the crystals. For example, the CN group in Y participates in weak intermolecular hydrogen bonds, whereas it does not in YN. Such effects can complicate the use of conformational polymorphism as a way to determine conformation–spectrum relationships.³²

Ab initio computational searches at the RHF/6-31G* level³³ for lowest energy conformers yielded two mirror-related structures with $\theta_{\text{thio}} = \pm 88.4^\circ$, $\theta_{\text{phen}} = \pm 174.6^\circ$, $\theta_{\text{nitro}} = \pm 0.7^\circ$. These structures resemble those observed in Y or YN, which contain perpendicularly related *o*-nitroaniline and amino thiophene fragments, each fragment being approximately planar. The potential energy (PE) as a function of θ_{thio} has two barriers (Figure 8): $\theta_{\text{thio}} = 0^\circ$ (7.3 kJ/mol) and 180° (15.3 kJ/mol). The $\theta_{\text{thio}} = 0^\circ$ structure contains the S atom *trans* to the amino hydrogen, whereas in the $\theta_{\text{thio}} = 180^\circ$ structure they are *cis* to each other. These barriers are insufficient for the separation of the opposite enantiomers of **1** at room temperature. In room-temperature solutions ($RT \approx 2.4$ kJ/mol), one expects a broad distribution of conformers, both perpendicular (major) and nonperpendicular (minor), with the nonperpendicular ones obtained by either increasing or decreasing θ_{thio} from $\theta_{\text{thio}} \approx 90^\circ$.

Figure 8 also shows an increase in the molecular dipole moment μ as θ_{thio} approaches 0° . This trend can be understood in terms of the vectors connecting the electron-donating (amino) and electron-withdrawing (nitro and cyano) groups: at $\theta_{\text{thio}} = 180^\circ$, the two vectors approximately oppose each other, producing a low molecular dipole, whereas at $\theta_{\text{thio}} = 0^\circ$, they make a more acute angle and a greater molecular dipole.

The solid circles in Figure 8 correspond to the energies and dipole moments of the crystal conformers, which were calculated by geometry optimization with θ_{thio} , θ_{phen} , and θ_{nitro} fixed at the crystal values.³⁴ The noncoincidence of the crystal points with the PE curve indicates residual but not excessive conformational strains caused by non-thiophene torsions (e.g., phenyl or nitro).

Effect of Crystallization on Molecular Conformation. With the aid of Figure 8, several effects of crystallization on molecular

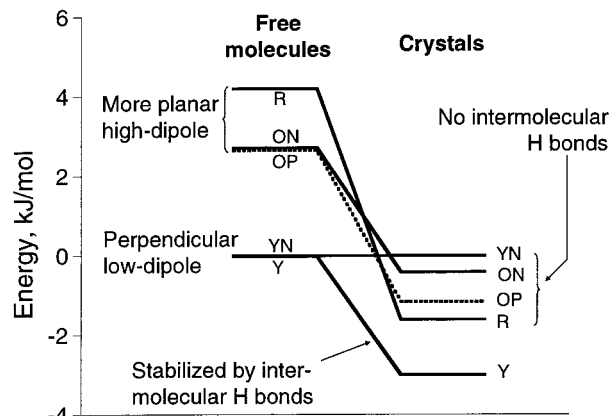


Figure 9. Comparison of conformational energies and crystal energies. YN = reference form.

conformation are recognized: the crystal conformers are not uniformly distributed on the PE curve but are situated either near the minima or on the $\theta_{\text{thio}} = 0^\circ$ side of the minima; conformer R, which is unstable in solutions, is selected for the construction of crystals; from two essentially identical conformers (Y and YN) grow crystals (Forms Y and YN) of the lowest and the highest energies among the polymorphs studied.

To assess the effect of crystal forces on molecular conformation quantitatively, we partitioned the energy difference between polymorphs into differences in conformational energy, ΔE_C , and lattice energy, ΔE_L : $\Delta E = \Delta E_C + \Delta E_L$. ΔE_L measures the energetic consequence of constructing crystals using different conformers. We calculated ΔE_L from ΔE , which is given by ΔH in Table 4,³⁵ and ΔE_C , which is obtained by ab initio calculations. For those polymorphs that do not contain intermolecular hydrogen bonds, crystallization has a stabilizing effect for the higher-energy conformers (ON, OP, and R) with $\Delta E_L = 3.1$, 3.8, and 5.8 kJ/mol, respectively (see Figure 9), over the lowest-energy conformer YN.

This trend can be attributed to two factors: favorable packing geometry of more planar conformers, and greater electrostatic interactions between larger dipoles. The close-packing explanation is consistent with the density data (Table 1). Molecules similar to **1** have been found to prefer planar geometries upon crystallization, even when they are not strongly polar.^{6–8,36} Since **1** has two planar structures ($\theta_{\text{thio}} = 0$ or 180°), the preference for low- θ_{thio} conformers requires an explanation. One reason

(34) Energies of crystal conformers were also calculated for molecules directly “removed” from crystals. Ideal in principle, this method yielded energies entirely unreasonable for single-bond rotamers (difference as much as 200 kJ/mol). This problem arose mainly from the H positions that are not well-determined by X-ray diffraction. To circumvent this problem, we “relaxed” the hydrogen atoms by geometry optimization with all heavy atoms frozen. Although this method produced energies that are reasonable for single-bond rotamers, a significant difference between conformers Y and YN (3.5 kJ/mol) was still considered too large, considering their nearly identical conformations. This difference might have arisen from slight strains caused by residual errors in heavy-atom coordinates, which need not be great to cause energy differences of such magnitude. The Y – YN difference vanished upon geometry optimization with only θ_{thio} , θ_{phen} , and θ_{nitro} fixed. We considered results thus obtained as a “true” measure of conformational energies of molecules observed in different polymorphs.

(35) At 1 atm, the difference between ΔH and ΔE , the enthalpy and energy differences between polymorphs, is negligible. This is seen from their relationship $\Delta H = \Delta E + P\Delta V$, where $P = 1$ atm and ΔV is the difference in molar volumes between two polymorphs. At room temperature, the $P\Delta V$ term for the polymorphic pair of Y (most dense) and ON (least dense) is (1 atm)($1/d_{\text{ON}} - 1/d_{\text{Y}}$) (259.29 g/mol) = 0.24 J/mol, which is much smaller than the ΔH values (several kJ/mol, see Table 4).

(36) Peterson, M. L.; Strnad, J. T.; Markotan, T. P.; Morales, C. A.; Scaltrito, V.; Staley, S. W. *J. Org. Chem.* **1999**, *64*, 9067–9076.

(32) Bernstein, J.; Anderson, T. E.; Eckhardt, C. J. *J. Am. Chem. Soc.* **1979**, *101*, 541–545.

(33) *Spartan 5.0*; Wavefunction, Inc., 18401 Van Karman Ave., #370; Irvine, CA 92715.

for this bias may be the higher conformational energy near $\theta_{\text{thio}} = 180^\circ$ than $\theta_{\text{thio}} = 0^\circ$. Another may be the greater dipole moments of low- θ_{thio} conformers, which are stabilized by dipole–dipole interactions.

The stabilization of high-dipole conformers is consistent with the red-shift of the CN band on going from a CCl_4 solution to the pure melt.³⁷ Enhanced dipole–dipole interactions in the melt are expected to stabilize high-dipole conformers or alternatively, lower the $\theta_{\text{thio}} = 0^\circ$ barrier, thus allowing a greater population of low- θ_{thio} conformers. An analogous effect has been observed with 1,2-dihaloethanes ($X = \text{Cl}, \text{Br}$), whose gauche (dipole bearing)-anti (zero dipole) energy difference is reduced upon liquefaction by approximately 3 kJ/mol.³⁸

Although they contribute insignificantly to the stability³⁹ and space-group preference⁴⁰ of certain organic crystals, dipole–dipole interactions may play a greater structure-determining role in the crystallization of **1** by virtue of its relatively large dipoles (6–8 D). Investigations of analogues of **1** revealed similar preferences for perpendicular conformers in solutions and planar, high-dipole conformers in crystals.⁴¹

The above explanation does not account for the stability of Form Y: although constructed from a perpendicular, low-dipole conformer, Form Y has the lowest energy among the polymorphs. This exception can be explained by the fact that Form Y alone contains intermolecular hydrogen bonds. These intermolecular hydrogen bonds are undoubtedly weak, since the amino hydrogen is already involved in an intramolecular hydrogen bond and the lattice energy of Form Y is less than 3 kJ/mol below the other polymorphs.⁴² However, even such weak intermolecular hydrogen bonds appear to reverse the stability trend established by purely van der Waals forces.

The Energy–Entropy Interplay. The relative importance of the energy and entropy contributions to the relative stability of polymorphs ($\Delta G = \Delta H - T\Delta S$) can be measured by the ratio $T\Delta S/\Delta H$, which is zero at 0 K (only ΔH important), 1 at

the transition temperature T_t (ΔH and $T\Delta S$ equally important), and > 1 above T_t ($T\Delta S$ more important). For the pair Y–R, $T\Delta S/\Delta H = 0.85$ at the melting point of R, indicating that although Form Y is still more stable, the entropy term is now a significant portion of the energy term. For the pairs Y–ON and Y–OP, at the melting point of Y, the entropy term has exceeded the energy term by approximately 10%, indicating a reversal of stability at some lower temperature.

Repeating the analysis at room temperature (using the same ΔH and ΔS values as in Table 4 and $T = 298 \text{ K}$), we found $T\Delta S/\Delta H = 0.67$ (R–Y), 0.88 (Y–OP), 0.87 (Y–ON). Thus, even though the entropy term has not overcome the energy terms at room temperature, the magnitude of the entropy terms is not negligible. This observation underscores the importance of including the entropy effect in the investigation of conformational polymorphism.

Conclusions

Several competing factors account for the complex stability relationships between the six polymorphs of **1**: the preference for perpendicular conformations in solutions, the preference for planar/high dipole conformers in crystals, the formation of intermolecular hydrogen bonds in Form Y alone, and the thermodynamic tendency toward low energy (provided by close packing) and high entropy (provided by more open structures). The interplay of these factors is likely the origin of an unusual degree of polymorphism displayed by this system.

From a practical point of view, the existence of at least six polymorphs within a small free-energy range and a broad conformational distribution in solutions and melt undoubtedly contribute to the poor polymorphic selectivity of crystallization and concomitant polymorphism. Given the poor thermodynamic selectivity, it would be interesting to investigate kinetic means through which polymorphic selectivity can be improved.

Acknowledgment. We thank P. Fanwick and the Purdue University Chemistry Department for the use of the X-ray crystallography facility and R. Vansickle, E. Groleau, and J. Osborne of Eli Lilly & Company for analytical assistance. This work was supported in part by the Joint Project for The Study of Mobility of Pharmaceutical Solids.

Supporting Information Available: Detailed crystallographic data, details on Cambridge Structural Database search on crystal polymorphs, and results of ab initio calculations (PDF). This material is available free of charge via the Internet at <http://pubs.acs.org>.

JA9930622

(37) The temperature at which the melt spectrum was measured (22 °C) is well above the glass transition temperature T_g of **1** (–13 °C), thus ensuring internal equilibrium in conformational distribution. T_g was measured by DSC at 10 °C/min using the standard melt/quench technique.

(38) Eliel, E. L.; Wilen, S. H. *Stereochemistry of Organic Compounds*; John Wiley & Sons: New York, 1994.

(39) Gavezzotti, A. *J. Phys. Chem.* **1990**, *94*, 4319–4325.

(40) Whitesell, J. K.; Davis, R. E.; Saunders, L. L.; Wilson, R. J.; Feagins, J. P. *J. Am. Chem. Soc.* **1991**, *113*, 3267–3270.

(41) Borchardt, T. Ph.D. Thesis, Purdue University, 1997.

(42) This energy difference is much smaller than the expected 10–20 kJ/mol from the formation of an intermolecular N–H···N bond (see, for example: Pimentel, G. C.; McClellan, A. L. *The Hydrogen Bond*; W. H. Freeman & Co.: San Francisco, 1960).